

## Resonant ion-dip infrared spectroscopy of benzene–(methanol) $m$ clusters with $m=1-6$

R. Nathaniel Pribble, Fredrick C. Hagemeister, and Timothy S. Zwier

Citation: *The Journal of Chemical Physics* **106**, 2145 (1997); doi: 10.1063/1.473784

View online: <http://dx.doi.org/10.1063/1.473784>

View Table of Contents: <http://scitation.aip.org/content/aip/journal/jcp/106/6?ver=pdfcov>

Published by the AIP Publishing

### Articles you may be interested in

IR spectroscopy on isolated  $\text{Co}_n(\text{alcohol})_m$  cluster anions ( $n = 1-4$ ,  $m = 1-3$ ): Structures and spin states  
*J. Chem. Phys.* **133**, 194304 (2010); 10.1063/1.3502096

Cooperativity of hydrogen-bonded networks in 7-azaindole ( $\text{C}_7\text{H}_5\text{N}_2\text{O}$ ) $_n$  ( $n = 2, 3$ ) clusters evidenced by IR-UV ion-dip spectroscopy and natural bond orbital analysis  
*J. Chem. Phys.* **129**, 054303 (2008); 10.1063/1.2961031

Infrared predissociation spectroscopy of  $\text{I}^-(\text{CH}_3\text{OH})_n$ ,  $n=1,2$ : Cooperativity in asymmetric solvation  
*J. Chem. Phys.* **116**, 4853 (2002); 10.1063/1.1451249

Behaviors of an excess proton in solute-containing water clusters: A case study of  $\text{H}^+(\text{CH}_3\text{OH})(\text{H}_2\text{O})_{1-6}$   
*J. Chem. Phys.* **112**, 176 (2000); 10.1063/1.480653

The hydrogen-bonding topologies of indole–(water)  $n$  clusters from resonant ion-dip infrared spectroscopy  
*J. Chem. Phys.* **108**, 3379 (1998); 10.1063/1.475356



# NEW Special Topic Sections

**NOW ONLINE**  
 Lithium Niobate Properties and Applications:  
 Reviews of Emerging Trends

**AIP** Applied Physics Reviews

# Resonant ion-dip infrared spectroscopy of benzene-(methanol)<sub>m</sub> clusters with $m=1-6$

R. Nathaniel Pribble, Fredrick C. Hagemeister, and Timothy S. Zwier<sup>a)</sup>  
Department of Chemistry, Purdue University, West Lafayette, Indiana 47907-1393

(Received 13 June 1996; accepted 7 November 1996)

Resonant ion-dip infrared spectroscopy has been employed to record cluster-size-specific spectra of  $C_6H_6-(CH_3OH)_m$  with  $m=1-6$  in the OH stretch fundamental region. The comparison of the spectra with the results of *ab initio* calculations on the pure methanol clusters enables the assignment of the hydrogen-bonding architecture in the clusters. In all cases, the methanol molecules aggregate together in a single subcluster. With  $m=1$ , a single infrared transition is observed, redshifted from that of a free methanol monomer by  $42\text{ cm}^{-1}$  due to  $\pi$  hydrogen bonding between benzene and methanol. The  $m=2$  spectrum features two strong transitions at  $3506$  and  $3605\text{ cm}^{-1}$ . The lower frequency peak is redshifted from the free monomer value by  $175\text{ cm}^{-1}$  and is assigned to the proton donor in the methanol dimer subcluster. The proton acceptor, which would be a free OH stretch in the absence of benzene, is redshifted by  $76\text{ cm}^{-1}$  due to a strengthened  $\pi$  hydrogen bond. In benzene- $(CH_3OH)_3$ , three sharp OH stretch transitions are observed at  $3389$ ,  $3435$ , and  $3589\text{ cm}^{-1}$ . The comparison of these absorptions with *ab initio* calculations and with experiments on the pure methanol trimer leads to a structure for benzene- $(CH_3OH)_3$  which incorporates a  $\pi$  hydrogen-bonded methanol trimer chain, confirming the earlier assignment based on its ultraviolet spectrum. The  $3589\text{ cm}^{-1}$  transition, due to the  $\pi$  hydrogen bond of the terminal methanol, is redshifted from the free monomer by  $93\text{ cm}^{-1}$ , a value approaching that of the donor methanol in methanol dimer ( $-107\text{ cm}^{-1}$ ). The lower frequency transitions in the  $m=3$  spectrum arise from the donor-acceptor and donor OH stretches in the methanol trimer chain. The spectral characteristics change when  $m=4$ . The OH stretch transitions are all located in a region around  $3320\text{ cm}^{-1}$  and are significantly broadened compared to the smaller clusters. By comparison with *ab initio* calculations, the methanol tetramer structure in benzene- $(CH_3OH)_4$  is deduced to be a cyclic methanol tetramer. The spectra for  $m=5$  and  $6$  are slightly redshifted but similar to  $m=4$  and point toward cyclic structures as well. © 1997 American Institute of Physics. [S0021-9606(97)02406-9]

## I. INTRODUCTION

As the prototypical aromatic hydrocarbon, benzene possesses two dissimilar regions for interaction with polar solvents; an electron-rich hydrophilic out-of-plane region created by its  $\pi$  cloud and a hydrophobic in-plane region generated by its aryl hydrogens. An evident manifestation of benzene's different interactions with seemingly similar solvents is its immiscibility in water and complete miscibility in methanol. An important aspect of these intermolecular interactions is the different hydrogen-bonding properties of the protic solvents themselves. Whether in the liquid,<sup>1</sup> solid,<sup>2</sup> or in large gas-phase clusters,<sup>3-6</sup> water is known to prefer three-dimensional hydrogen-bonded networks. Methanol, in contrast, forms H-bonded chains as a solid,<sup>7</sup> and is thought to prefer such chains in the liquid<sup>8</sup> as well. At the same time, data on the pure gas phase methanol clusters<sup>9-12</sup> with  $n=3-5$  suggest the formation of cyclic structures which maximize the number and strength of the methanol-methanol H-bonds. The interactions of these different H-bonding architectures with benzene, and the disruption caused by benzene in the network of H-bonds, undoubtedly play a significant role in the different solubilities of benzene in water and methanol.

The study of the gas-phase clusters of benzene with water and methanol can provide critical tests of the intermolecular potentials involved, which, it is hoped, will lead to a better molecular-scale understanding of the bulk solutions themselves. Much of the work that has been done on benzene-(water)<sub>n</sub> and benzene-(methanol)<sub>n</sub> clusters probes the perturbations imposed by the solvent molecules on the electronic spectrum of benzene.<sup>13-15</sup> Size selection of the clusters is typically accomplished in these studies using resonant two-photon ionization (R2PI) coupled with time-of-flight mass spectroscopy (TOFMS). Our group used a combination of rotational band contour analysis and vibronic level arguments to study benzene-(H<sub>2</sub>O)<sub>n</sub> clusters<sup>13</sup> (denoted BW<sub>n</sub>) with  $n=1-8$  and benzene- $(CH_3OH)_m$  clusters<sup>14</sup> (denoted BM<sub>m</sub>) with  $m=1-5$ . The vibronic level probes used in these studies took advantage of the high symmetry of benzene and the forbidden nature of the  $S_1 \leftarrow S_0$  transition in isolated benzene. In the presence of solvent molecules, this symmetry is reduced, turning on new transitions (e.g., the origin) and splitting degeneracies (e.g., the  $e_{2g}\nu_6$  vibration) in benzene's spectrum. Among the vibronic level probes of the cluster structure were the vibronic frequency shift, the extent of fragmentation induced by photoionization, the presence of van der Waals absorptions, the  $0_0^0/6_0^1$  intensity ratio, and the magnitude of the  $6_0^1$  splitting. The vibronic spectroscopy

<sup>a)</sup> Author to whom all correspondence should be addressed.

copy provides evidence that the water or methanol molecules in these clusters form a  $W_n$  or  $M_n$  subcluster containing all the solvent molecules in a single H-bonded aggregate, but provides only circumstantial evidence for the H-bonded structure of the  $W_n$  or  $M_n$  subclusters themselves.

In the  $BM_m$  clusters of interest here, the R2PI spectra<sup>14</sup> [reproduced in Figs. 1(a)–(d)] suggest that the methanol molecules in  $BM_m$  when  $m=1$ –3 are H-bonded chains which retain the  $\pi$  hydrogen bond with benzene, while  $m=4$  and 5 do not possess a  $\pi$  H bond and therefore were suggested to be cyclic. This was most notably evident in the vibronic frequency shifts of the transitions relative to free benzene (Fig. 1), which are increasingly blueshifted through  $m=3$  due to the  $\pi$  H bond, but shift dramatically back to the red in  $m=4$  and 5.

In the present paper we test these tentative structural conclusions much more directly by recording infrared spectra of the clusters in the OH stretch region. In hydrogen bonded molecules ( $Y\cdots HX$ ), the H–X stretching vibration is one of the more powerful and sensitive probes of the intermolecular hydrogen bond. The OH stretch is sensitive to the strength, type, and number of hydrogen bonds in which it participates because it vibrates directly against the hydrogen bond. When a hydrogen bond is present, the H–X stretch fundamental shifts its frequency to the red, increases in breadth, and typically increases in intensity.<sup>16,17</sup>

In the condensed phase,<sup>18</sup> the observed consequence of the extended H-bonded networks on the OH stretch absorption band is its enormous breadth, typically extending from 3700 to 3100  $cm^{-1}$ . Liquid methanol in particular has a strong, broad, and essentially featureless OH stretch band peaked at 3337  $cm^{-1}$  while solid methanol's OH stretch absorption shows substructure peaked at 3187 (s) and 3284  $cm^{-1}$  (vs), with a shoulder at 3443  $cm^{-1}$ .<sup>18</sup>

By studying the expansion-cooled, gas-phase clusters, one hopes to probe the OH stretch absorptions of conformation- and size-specific H-bonded aggregates with sufficient resolution to observe the individual OH stretch bands “underneath” the broad absorption present in the condensed phase. Recently, using a pulsed tunable IR source in combination with R2PI-time-of-flight mass spectrometer (TOFMS) our group<sup>3–5,19</sup> probed the OH stretch region of size-specific hydrogen-bonded  $BW_n$  clusters with  $n=1$ –7 using a technique first developed by Page, Shen, and Lee<sup>20</sup> which we call resonant ion-dip infrared spectroscopy (RIDIRS). In RIDIRS, the absorption of an infrared photon removes population from the ground state and is detected by a decrease in the mass-selected ion signal produced by a fixed UV laser tuned to a given vibronic transition of the cluster of interest. Figure 2(B) reproduces the RIDIR spectra of  $BW_n$  with  $n=1$ –7. These spectra will serve as a point of comparison with the present results on  $BM_m$ . In the work on  $BW_n$ , the interaction between benzene and the  $W_n$  subcluster is always found to be through a  $\pi$  H bond. The comparison of the spectra with *ab initio* calculations on  $BW_n$  and  $W_n$  clusters provide clear assignments for the H-bonding structure of the clusters. The  $BW_n$  clusters with  $n=3$ –5 are seen to have cyclic  $W_n$  subclusters, while the spectra of the  $n=6$

and 7 clusters were assigned to  $\pi$  H-bonded  $W_n$  subclusters which were three-dimensional, H-bonded networks containing several “double donor” water molecules.<sup>3–5,19</sup>

Using the same technique, the emphasis of this study is the OH stretch region of  $BM_m$  ( $m=1$ –6) clusters. We will demonstrate that the predictions previously made through the  $S_1 \leftarrow S_0$  spectroscopy of the clusters<sup>13,14</sup> are correct; namely, (i) that the  $BM_m$  clusters with  $m=1$ –3 form H-bonded chains which retain the  $\pi$  H bond to benzene, and (ii) that the larger  $BM_m$  clusters contain a cyclic  $M_m$  subcluster. The *ab initio* calculations of the structures, vibrational frequencies, and infrared intensities of the pure  $M_m$  clusters, which are presented in detail elsewhere,<sup>21</sup> (and hereafter referred to as paper I) play an important role in arriving at these conclusions. We shall also see that the presence of benzene and its perturbative effect on the  $M_m$  cluster are evident in the IR spectra of the clusters, and interpretable in terms of reasonable distortions of the  $M_m$  subcluster.

## II. EXPERIMENT

RIDIR spectra in the OH stretch region are recorded using methods described previously.<sup>3–5,19</sup> Briefly, cold, gas-phase  $BM_m$  clusters are formed by expanding a mixture containing benzene and methanol in helium from a pulsed valve of 0.8 mm diam operating at 20 Hz. The concentration of these vapors is controlled by metering the flows of helium over the room temperature liquids using needle valves and mixing these flows with a balance of helium. Typical expansion conditions employ 0.1% benzene and 0.1%–0.5% methanol at a total pressure of 2 bar. The clusters are passed through a skimmer, located 4 cm downstream from the pulsed nozzle, and into the ion-source region of the time-of-flight mass spectrometer (TOFMS), where the cluster of interest is singled out for study using resonant two-photon ionization (R2PI) through its  $S_1 \leftarrow S_0 6_0^1$  transition. The pulsed ultraviolet laser (0.1–0.5 mJ/pulse) used for the R2PI traverses twice through the ionization region of the TOFMS in a 1-mm-diam collimated beam. The ions of equal mass created from the two passes are born at slightly different potentials in the ion source and arrive at the microchannel plate ion detector as two ion packets separated by 100–200 ns. The arrival times of the ion mass of interest are monitored with a digital oscilloscope. The pulsed, tunable IR output of an optical parametric oscillator (OPO)<sup>19</sup> is spatially overlapped with one of the UV beams while temporally preceding the UV pulse by 80–400 ns. When an IR absorption occurs out of the same ground state level as that monitored in R2PI, a decrease in ion signal from the overlapped UV beam is observed. Normalization of the two ion signals allows the percent depletion in ion signal as a function of OPO wavelength to be attained. The dual-beam method reduces the noise arising from shot-to-shot UV laser power fluctuations.

Typical idler pulse energies of 1–3 mJ/pulse are used. The OPO power curve over the frequency range of interest is included above the RIDIR spectra of Fig. 2(A). The dip in idler power over the 3460–3510  $cm^{-1}$  region is due to an impurity absorption in the  $LiNbO_3$  crystal, which in the

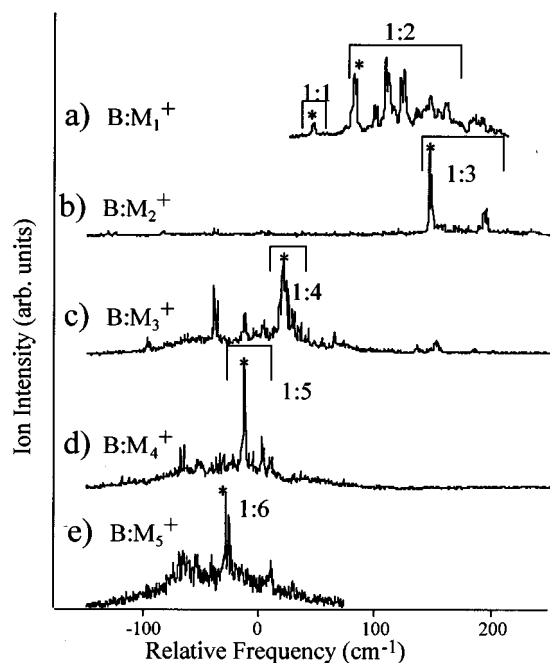


FIG. 1. One-color resonant two-photon ionization scans of  $BM_m$  clusters with  $m=1-6$  in the  $6_0^1$  region of the  $S_1 \leftarrow S_0$  transition of benzene. Efficient fragmentation occurs following photoionization by loss of one methanol so that the  $BM_m$  cluster is monitored in the  $BM_{m-1}^+$  mass channel. See Ref. 14 for details of the assignments. 1: $m$  designates the  $B_1M_m$  cluster. The bands marked with asterisks are those monitored in recording resonant ion-dip infrared spectra.

present crystal is more substantial than in the  $BW_n$  spectra [Fig. 2(B) top]. While the idler power is not zero in this region, it is small enough that absorptions in this region are significantly reduced in intensity. The RIDIR spectra are not corrected for the wavelength dependence of the OPO power.

The observed depletions are necessarily large, approaching 50% in some cases. In our previous work on  $BW_n$  clusters<sup>3-5,19</sup> [reproduced in Fig. 2(B)], even larger depletions were observed. In all the spectra of Fig. 2, vibrational predissociation or hydrogen-bond breaking in the cluster may be occurring following  $OH(\nu=1)$  excitation, allowing depletions greater than 50% to occur. Given the large depletions observed, saturation effects will distort the relative intensities in the spectra by artificially raising the intensity of weak transitions relative to strong ones.

### III. RESULTS

#### A. R2PI spectra

As mentioned earlier, Figs. 1(a)–1(d) reproduce the one-color R2PI spectra reported in our previous work<sup>14</sup> on  $BM_m$  clusters. The assignments for the cluster sizes responsible for the observed transitions are given in Fig. 1. The  $BM_m$  clusters undergo efficient fragmentation following photoionization by loss of a single methanol molecule. Support for these assignments has been given elsewhere.<sup>14</sup> The transitions marked with an asterisk in Fig. 1 are used to selectively monitor the indicated  $BM_m$  cluster in the RIDIR spectra. The

additional transitions in the  $BM_3^+$  mass channel have recently been assigned to conformational isomers of  $B_2M_3$  clusters.<sup>22</sup>

The R2PI spectrum of  $BM_6$ , shown in Fig. 1(e), has not been reported previously. The spectrum is dominated by a doublet at  $-27\text{ cm}^{-1}$  which we assign to  $BM_6$ . There are undoubtedly contributions to the broad background in the spectrum from larger clusters. The spectrum of  $BM_6$  has an unmistakable resemblance to the spectrum of the “stem” benzene in the benzene dimer.<sup>23</sup> The  $-27\text{ cm}^{-1}$  frequency shift continues the trend set in  $BM_4$  and  $BM_5$  toward increasing redshift, which here approaches the value of  $-41\text{ cm}^{-1}$  for the benzene dimer stem molecule. Like  $BM_5$ , little van der Waals’s structure is evident in the spectrum of  $BM_6$ . The  $6_0^1$  splitting in  $BM_6$  is  $3.2\text{ cm}^{-1}$ , indicating that the six-fold symmetry of benzene has been broken to lower than three-fold symmetry by the  $M_6$  subcluster.

#### B. RIDIR spectra

Overview RIDIR spectra of the  $BM_m$  ( $m=1-6$ ) clusters in the OH stretch region are shown in Fig. 2(A), spectra (a) and (f). The frequencies of the transitions are listed in the first column of Table I. Assignments of the features in Fig. 2(A) are given in the last column of Table I and will be considered later. The RIDIR spectra for each cluster size in Fig. 2(A) were obtained by monitoring the ion signal that resulted from the R2PI laser being fixed on the peak maximum of the  $6_0^1$  transition of the given cluster [indicated by an asterisk in Fig. 2(A)] while scanning the IR OPO frequency.

The general development of the RIDIR spectra with cluster size reflects the sensitivity of the methanol molecule to its hydrogen-bonding environment. The key spectral features of the smaller clusters ( $m=1-3$ ) are as follows. First, a transition around  $3600\text{ cm}^{-1}$  appears in each of the spectra, which is redshifted by about  $20\text{ cm}^{-1}$  with the addition of each successive methanol molecule. Second, the lowest-frequency transitions shift about  $125\text{ cm}^{-1}$  further to the red with the addition of each methanol molecule, to a lowest frequency of  $3389\text{ cm}^{-1}$  in  $BM_3$ . Third, the transitions are quite narrow, ranging from 2.8 to  $7.7\text{ cm}^{-1}$  full width at half-maximum (FWHM).

These features of the smaller clusters’ spectra are in sharp contrast with the  $m=4-6$  data. First, in these larger clusters, the transition around  $3600\text{ cm}^{-1}$  is notably absent. Second, the frequency shift of the transitions which are observed change far less with increasing cluster size than their smaller counterparts. With the addition of the fifth methanol, the maximum absorption shifts just  $60\text{ cm}^{-1}$  from the  $m=4$  cluster center frequency, while the addition of the sixth methanol molecule shifts the center frequency by only about  $20\text{ cm}^{-1}$  further. Third, the widths of the majority of transitions are approximately  $30\text{ cm}^{-1}$ , almost an order of magnitude greater than the widths in the smaller clusters. Finally, the transitions span an O–H spectral region from  $3360$  to  $3150\text{ cm}^{-1}$ . This encompasses the peak maxima observed in the O–H stretch region in liquid and solid methanol.

TABLE I. Experimental and calculated OH stretch frequencies ( $cm^{-1}$ ), frequency shifts ( $cm^{-1}$ ), and assignments for  $C_6H_6-(CH_3OH)_m$  and  $(CH_3OH)_m$  clusters.

	Expt. <sup>a</sup>		Calc. <sup>b</sup> C <sub>6</sub> H <sub>6</sub> -(CH <sub>3</sub> OH) <sub>m</sub> Δν	Expt. (CH <sub>3</sub> OH) <sub>m</sub>		N <sub>2</sub> matrix <sup>d</sup> ν	Calc. <sup>b</sup> (CH <sub>3</sub> OH) <sub>m</sub> Δν	Assignment
	C <sub>6</sub> H <sub>6</sub> -(CH <sub>3</sub> OH) <sub>m</sub>			Gas phase <sup>c</sup>				
	ν	Δν		ν	Δν			
m = 1	3639	−42	−33	3681.5		3640	0	πH bond Free O–H
m = 2	3506( <i>s</i> )	−175	−189( <i>s</i> )	3574.4( <i>s</i> )	−107	3504	−150( <i>s</i> )	M–M H bond
	3605( <i>s</i> )	−76	−57( <i>s</i> )	3684.1( <i>w</i> )	+3	3654	−4( <i>w</i> )	πH bond Free O–H
	3640( <i>w</i> )	−41						
m = 3				3462( <i>s</i> )	−219	3440–3450	−297( <i>w</i> )	Cyclic
							−241( <i>s</i> )	
							−228( <i>s</i> )	
	3389( <i>s</i> )	−292				3389.2	−259( <i>s</i> )	Chain
	3435( <i>s</i> )	−246				3433.3	−208( <i>s</i> )	second M–M H bond
	3589( <i>s</i> )	−92						first M–M H bond
						3661.94	+13( <i>s</i> )	πH bond Free O–H
m > 3				3290	−391			Higher polymers
m = 4	3204( <i>w</i> )	−477					−462( <i>w</i> )	Cyclic
	3290( <i>s</i> )	−391				3284	−371( <i>s</i> )	
	3321( <i>s</i> )	−360					−371( <i>s</i> )	
	3360( <i>w</i> )	−321					−334( <i>w</i> )	
m > 4						3220		Higher polymers
						3242		
						3260		
m = 5	3171( <i>w</i> )	−510					−504( <i>w</i> )	Cyclic
	3243( <i>s</i> )	−438					−425( <i>s</i> )	
	3286( <i>w</i> )	−395					−414( <i>s</i> )	
	3314( <i>w</i> )	−367					−358( <i>w</i> )	
							−358( <i>w</i> )	
m = 6	3177	−504						Cyclic
	3224	−457						
	3280	−401						
	3315	−366						

<sup>a</sup>Results from this work.<sup>b</sup>Harmonic frequencies at the DFT Becke3LYP/6-31+G\* level of theory. Frequency shifts are reported with respect to methanol monomer's OH stretch.<sup>c</sup>Reference 11.<sup>d</sup>Reference 23.

### C. Density functional theory calculations

In addition to the extensive calculations from paper I on the pure  $M_m$  clusters,<sup>21</sup> we have carried out calculations of the structures, binding energies, vibrational frequencies, and infrared intensities of  $BM_1$  and  $BM_2$  at the same level of theory as in that work [density functional theory (DFT) Becke3LYP/6-31+G\*]. Corresponding calculations on larger  $BM_m$  clusters were not carried out due to the increasing complexity and length of the calculations. Figures 3(a) and 3(b) show pictorially the fully optimized structures for the clusters. The prediction of the calculation is that, as in  $BW_1$  and  $BW_2$ , the  $BM_1$  and  $BM_2$  clusters are both  $\pi$  H

bonded to benzene, with the  $M_2$  subcluster in  $BM_2$  largely retaining the structure of the free methanol dimer when in the presence of benzene.

A Becke3LYP/6-31+G\* binding energy of  $D_e = -2.4$  kcal/mol was calculated for the  $BM_1$  complex. In this optimized structure, methanol is  $\pi$  H bonded to benzene with an oxygen-to-benzene plane distance of 3.41 Å. The calculated frequency shift of the methanol OH stretch in  $BM_1$  is  $-33$   $cm^{-1}$  (Table I). As a comparison of the relative strength of the  $\pi$  H bond present in the  $BM_1$  complex, the methanol dimer possesses a calculated binding energy of  $D_e = 6.3$  kcal/mol and a calculated OH stretch frequency shift of  $-150$

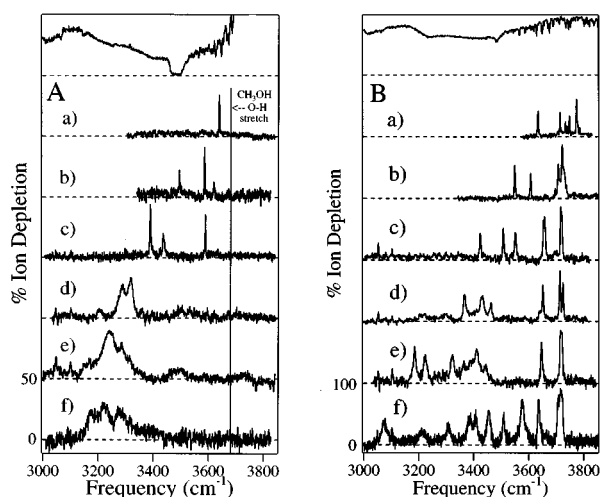


FIG. 2. (A) Overview RIDIR spectra of  $BM_m$  with (a)  $m=1$  to (f) 6, respectively. The vertical line indicates the frequency of the OH stretch in methanol monomer ( $3681\text{ cm}^{-1}$ ). (B) Analogous RIDIR spectra of  $BW_n$  with (a)  $n=1$  to (f) 6, respectively, for comparison. The top most trace on each figure is the OPO power curve for the  $LiNbO_3$  crystal used for the study. The spectra have not been corrected for OPO power.

$\text{cm}^{-1}$  at the same level of theory (paper I). The  $BM_1$  calculation predicts that the methanol molecule is pulled off the sixfold axis of benzene, presumably in order to gain additional interaction of the methyl group with the  $\pi$  cloud. The degree of nonrigidity of this complex has not been tested by calculation, but one might expect that the methanol molecule experiences only a small barrier to internal rotation about benzene's sixfold axis.

Several results from the  $BM_2$  calculation suggest a cooperative strengthening of the H bonds in  $BM_2$  relative to those in the dimeric subclusters  $BM_1$  and  $M_2$ . First, in  $BM_2$  the O–O distance decreases by  $-0.024\text{ \AA}$  from its value in the free methanol dimer ( $2.862\text{ \AA}$ ). Second, the calculated  $\pi$  H-bond distance in  $BM_2$  is  $0.019\text{ \AA}$  shorter than in  $BM_1$ .

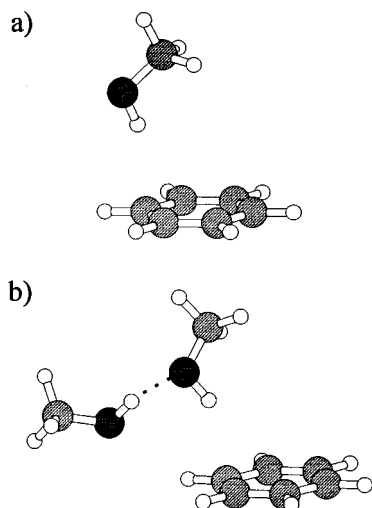


FIG. 3. Minimum energy structures calculated for (a)  $BM$  and (b)  $BM_2$  using the DFT Becke3LYP/6-31+G\* level of theory.

Third, the total binding energy of  $BM_2$  is  $-14.6\text{ kcal/mol}$ , over  $6\text{ kcal/mol}$  greater than the sum of the calculated  $BM_1$  ( $-2.2\text{ kcal/mol}$ ) and  $M_2$  ( $-6.28\text{ kcal/mol}$ ) binding energies at the same level of theory. Finally, the calculated OH stretch frequency shifts of the donor and  $\pi$  H-bonded methanol molecules from their monomer values are  $-190$  and  $-58\text{ cm}^{-1}$ , respectively, values which are significantly greater than those calculated for the corresponding vibrations in  $M_2$  ( $-150\text{ cm}^{-1}$ ) and  $BM_1$  ( $-33\text{ cm}^{-1}$ ), respectively.

#### IV. DISCUSSION

In analyzing the RIDIR spectra of the  $BM_m$  clusters, IR data on the  $M_m$  clusters provide excellent points of comparison. Table I list the observed O–H stretch absorptions in  $BM_m$  and compares these absorptions to gas-phase data,<sup>11</sup> matrix data,<sup>24</sup> the *ab initio* calculations on pure methanol clusters from paper I, and the analogous calculations on the two smallest  $BM_m$  clusters. The comparison of the present data on  $BM_m$  [Fig. 2(A)] with corresponding data<sup>3–5,19</sup> on  $BW_n$  will also be made in order to assess the similarities and differences which exist.

##### A. $C_6H_6-(CH_3OH)$

The RIDIR spectrum of  $BM_1$  [Fig. 2(A), spectrum (a)] is composed of a single absorption in the O–H stretch region at  $3639\text{ cm}^{-1}$ . This transition is  $42.5\text{ cm}^{-1}$  redshifted from the free methanol OH stretch ( $3681.5\text{ cm}^{-1}$ ) and is assigned to a  $\pi$  H-bonded OH stretch. This is consistent with the *ab initio* structure calculated for  $BM_1$ . In fact, the calculated redshift of the OH stretch ( $-33\text{ cm}^{-1}$ ) is in good agreement with that observed experimentally. No combination bands are observed.

There is little apparent similarity between the RIDIR spectra of  $BM_1$  and  $BW_1$  [Fig. 2(B), spectrum (a)]. If the  $BW$  complex were rigid, its OH stretch RIDIR spectrum would consist of two transitions due to its symmetric and antisymmetric stretch. Such a simple spectrum is in fact observed in  $B_2W_1$  (Ref. 22) and fluorobenzene- $W_1$ .<sup>25</sup> However, in the case of  $BW_1$ , at least seven resolved transitions are observed.<sup>19</sup> The four most intense transitions are assigned to OH stretch/internal rotation combination bands created by the nearly free internal rotation of the water about benzene's sixfold axis. The weaker transitions are assigned to OH stretch/in-plane torsion combination bands. Based on these assignments, center frequencies for the symmetric and asymmetric stretches of water in  $BW_1$  are computed to be  $23$  and  $25\text{ cm}^{-1}$  redshifted, respectively, from their frequencies in the water monomer.

Methanol, with its single OH functional group and “bulky” methyl group, forms a complex with benzene in which the OH orientation is significantly more constrained than in  $BW_1$ , thereby producing an uncongested spectrum that is characterized by its single  $\pi$  H-bonded OH absorption. The somewhat greater frequency shift ( $-43\text{ cm}^{-1}$ ) in  $BM_1$  than in  $BW_1$  ( $-23/-25$ ) may be ascribed to a strengthened  $\pi$  H bond associated with the increased polarizability of  $CH_3OH$  and a more highly directed  $\pi$  H bond involving a

single OH group. The lack of combination bands due to the internal rotation of methanol, which are so prevalent in the benzene–H<sub>2</sub>O spectrum [Fig. 2(B), spectrum (a)] may be largely a consequence of the much smaller internal rotation constant for methanol by comparison to H<sub>2</sub>O.

### B. $C_6H_6-(CH_3OH)_2$

Figure 4(c) presents a close-up of the RIDIR spectrum of BM<sub>2</sub>, with its three transitions at 3506, 3605, and 3640 cm<sup>-1</sup>. The small intensity of the lowest-frequency transition is an artifact of the low OPO power in the 3460–3510 cm<sup>-1</sup> region mentioned previously. Upon correction for this reduced power, the 3506 cm<sup>-1</sup> band is several times as intense as the 3605 cm<sup>-1</sup> band. The donor and acceptor OH stretch absorptions of gas phase methanol dimer have been identified<sup>11</sup> at 3574.4 and 3684.1 cm<sup>-1</sup>, respectively (Table I). In a nitrogen matrix,<sup>23,26,27</sup> the same absorptions occur around 3504 and 3654 cm<sup>-1</sup>. In Figs. 4(a) and 4(b), the calculated infrared spectra of the methanol dimer and of BM<sub>2</sub> are shown for comparison with the experimental spectrum of BM<sub>2</sub>. Based on these comparisons, we assign the band at 3506 cm<sup>-1</sup> to the donor OH stretch and that at 3605 cm<sup>-1</sup> to the  $\pi$  H-bonded OH stretch of a distorted methanol dimer in BM<sub>2</sub>, as shown in Fig. 3(b).

The donor transition (3506 cm<sup>-1</sup>) is redshifted by 79 cm<sup>-1</sup> from its value in the free methanol dimer, while the shift of the  $\pi$  H-bond transition (–76 cm<sup>-1</sup>) is nearly twice its value in BM<sub>1</sub> (–42 cm<sup>-1</sup>). As anticipated by the *ab initio* calculations, the magnitude of these shifts suggests significant cooperative strengthening of the  $\pi$  H bond and methanol–methanol H bond in the BM<sub>2</sub> cluster relative to those in BM<sub>1</sub> and M<sub>2</sub>, respectively. In the previous R2PI study of BM<sub>m</sub>,<sup>14</sup> it was suggested that the increase in the strength of the  $\pi$  hydrogen bond is responsible for the further blueshift in the vibronic transitions of BM<sub>2</sub> relative to BM<sub>1</sub> in the UV spectrum of Fig. 1(a).

The weak absorption at 3640 cm<sup>-1</sup> cannot be an OH stretch fundamental, but must instead be a combination band of one of the OH stretch bands with an intermolecular vibration of the BM<sub>2</sub> cluster. If this intermolecular mode is built on the  $\pi$  H-bonded OH, its frequency is about 35 cm<sup>-1</sup>. The intense intermolecular structure in the R2PI spectrum of BM<sub>2</sub> [Fig. 1(a)] includes strong bands at 28 and 41 cm<sup>-1</sup>, either of which could have a corresponding frequency in S<sub>0</sub> at 35 cm<sup>-1</sup>. Furthermore, it is physically reasonable that the 35 cm<sup>-1</sup> combination band is built off the  $\pi$  H-bonded OH stretch which is responsible for perturbing the benzene molecule in the R2PI spectrum.

Based on the RIDIR spectra, the structures of BM<sub>2</sub> and BW<sub>2</sub> are quite similar, incorporating a methanol or water dimer in which the acceptor molecule is  $\pi$  H bonded to benzene. The donor O–H stretch transitions of BM<sub>2</sub> and BW<sub>2</sub> are at 3506 and 3550 cm<sup>-1</sup>, respectively, corresponding to frequency shifts of –175 and –156 cm<sup>-1</sup> from their respective monomer's free OH stretch. The somewhat larger frequency shift in BM<sub>2</sub> is probably reflecting the slightly stronger H bond in M<sub>2</sub> than in W<sub>2</sub>. No ready comparison can

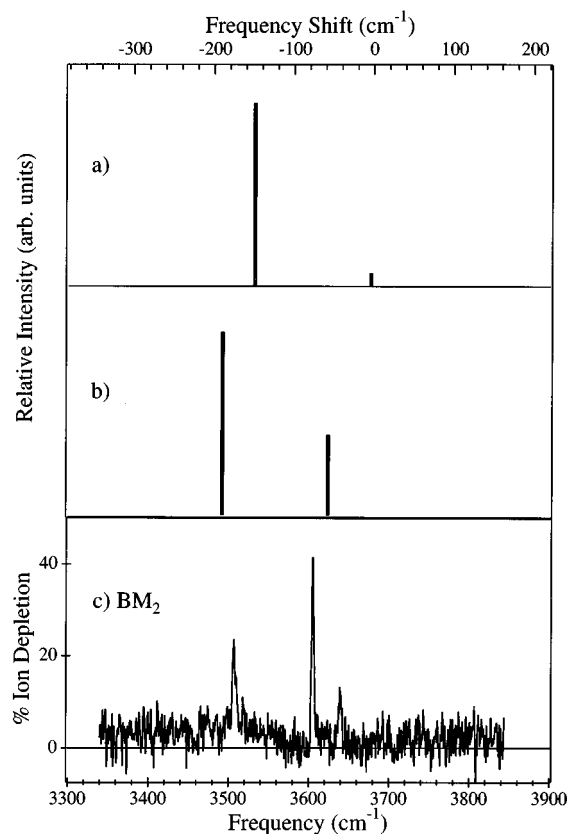


FIG. 4. (a) and (b) Calculated OH stretch harmonic frequency shifts and infrared intensities for the free methanol dimer (a) and BM<sub>2</sub> (b). (c) RIDIR spectrum of BM<sub>2</sub> for comparison.

be made between the  $\pi$  H-bonded OH stretch modes of BM<sub>2</sub> and BW<sub>2</sub>, because the acceptor water in BW<sub>2</sub> probably interacts with benzene's  $\pi$  cloud through both its hydrogens.<sup>13</sup>

### C. $C_6H_6-(CH_3OH)_3$

Based on the *ab initio* calculations of the methanol trimer from paper I, it is apparent that the methanol trimer has several conformational structures which could bind to benzene, including cyclic [(3)], chain [3], and branched [2+1] H-bonded structures. The notation for the M<sub>m</sub> structures is that introduced in paper I, in which cyclic clusters are designated by parentheses (*m*), chain structures by an underlined *m*, and branched-cyclic and branched-chain structures with a branch of *n* methanols by (*m*) + *n* and *m* + *n*, respectively. As shown in paper I, in the free methanol trimer the lowest energy structure predicted by calculation is that observed experimentally;<sup>9–11,23</sup> namely, the cyclic trimer. For this structure, Huisken *et al.*<sup>11</sup> have observed a single OH stretch band at 3462 cm<sup>-1</sup>. However, in a matrix,<sup>23</sup> the cyclic trimer breaks a H bond under infrared irradiation to form a chain methanol trimer with absorptions at 3661.94, 3433.3, and 3389.2 cm<sup>-1</sup>.

The two lower-frequency transitions observed in BM<sub>3</sub> (3389 and 3435 cm<sup>-1</sup>) match the matrix-isolated open chain trimer's absorptions to within 2 cm<sup>-1</sup>. The highest frequency OH stretch fundamental at 3589 cm<sup>-1</sup> in BM<sub>3</sub> is shifted by

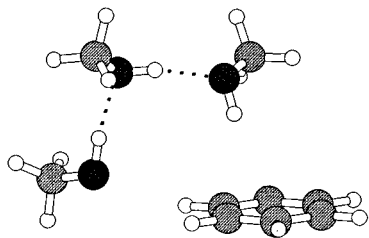


FIG. 5. A schematic picture of the  $BM_3$  “hydrogen-bonding” structure which is determined from the RIDIR spectroscopy. The structure includes a methanol trimer chain (3) with two methanol–methanol H bonds and a  $\pi$  H bond with benzene.

$-73\text{ cm}^{-1}$  from the end-of-chain methanol’s OH stretch frequency in the matrix-isolated chain trimer, a shift which is easily accounted for if the methanol trimer chain attaches to the  $\pi$  cloud of benzene through the only free OH available in the chain, as pictured schematically in Fig. 5. This is the same structure deduced from the R2PI spectroscopy for  $BM_3$  previously,<sup>14</sup> but now RIDIR spectroscopy provides more direct evidence to support that deduction.

As shown in Fig. 6, the DFT calculations from paper I on the cyclic and open chain methanol trimers confirm the distinct spectral signatures of cyclic and chain  $M_3$  and the better match of the latter structure with the experimental spectrum of  $BM_3$ . The calculated transitions shown in Figs. 6(a) and 6(b) are shown as frequency shifts from the methanol monomer OH stretch ( $3681.5\text{ cm}^{-1}$ ). Both the redshift in the highest-frequency OH stretch transition in  $M_3$  compared to  $BM_3$  and its greatly increased intensity are due to formation of the  $\pi$  H bond in the latter cluster. Note that the intensity of the  $\pi$  H-bonded OH stretch even approaches that of the OH groups in the  $M_3$  chain.

The experimental spectrum of  $BM_3$  also differs from the calculated spectrum for  $\bar{3}$  in its reversal of the relative intensities of the two lower-frequency OH stretch transitions. The calculated normal modes for  $\bar{3}$  from paper I indicate a local mode OH composition which is 80%/20% localized on the terminal/interior methanol for the lowest frequency transition ( $-259\text{ cm}^{-1}$ ) and 20%/80% for the  $-203\text{ cm}^{-1}$  transition. Since we do not have calculations for  $BM_3$  (due to their size), we can only suggest that the degree of delocalization of these modes may be altered in the presence of benzene, leading to the observed change in intensity.

It is interesting to compare the spectra and structures of  $BM_3$  and  $BW_3$  in Fig. 2(A), spectrum (c) and Fig. 2(B), spectrum (c), respectively. In  $BW_3$ , RIDIR spectroscopy<sup>3,4,20</sup> has shown that the water trimer is cyclic, while in  $BM_3$  the methanol trimer takes on a H-bonded chain structure. In the absence of benzene, both  $W_3$  and  $M_3$  have a cyclic lowest-energy structure. These cyclic structures have highly nonlinear H bonds which are thereby weakened,<sup>19(b),21</sup> however, the ring strain is more than compensated by gaining a third H bond in the cyclic structure by comparison to the two linear H bonds in the chain trimer. In the presence of benzene, the water trimer retains its cyclic structure because it can  $\pi$  H bond to benzene via one of its free OH groups. This weak  $\pi$

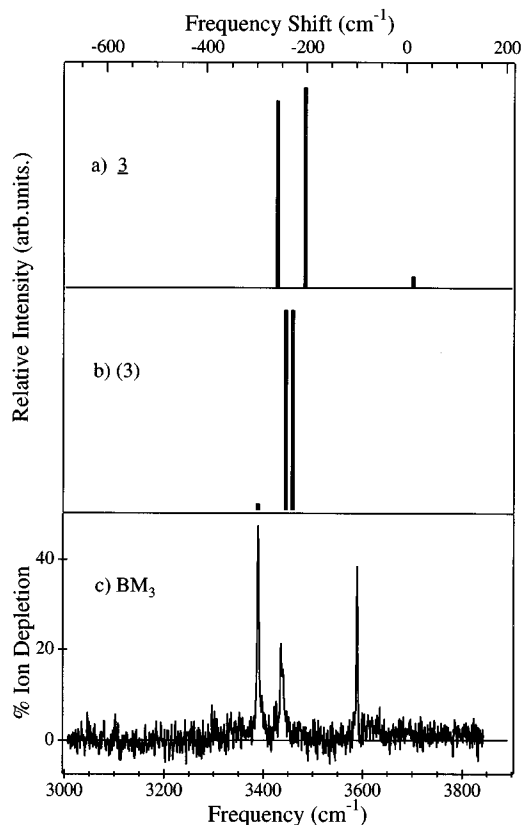


FIG. 6. (a) and (b) Calculated OH stretch harmonic frequency shifts and infrared intensities for the chain (a) and cyclic forms (b) of the free methanol trimer. (c) RIDIR spectrum of  $BM_3$  for comparison.

H bond shifts one of the free OH stretch frequencies by about  $60\text{ cm}^{-1}$  [Fig. 2(B), spectrum (c)]. In addition, the benzene molecule asymmetrizes the cyclic water trimer structure enough that (i) the degeneracy of the two single donor OH vibrations which carry IR intensity in  $W_3$  is split, and (ii) intensity is induced in the lowest-frequency single donor OH stretch which is forbidden in  $W_3$ .

In contrast, in  $BM_3$ , the presence of benzene reverses the stabilities of the cyclic and chain methanol trimers. The cyclic methanol trimer, which has no free OH’s available for  $\pi$  H bonding, is destabilized by its weak interaction with benzene. Instead, the chain  $M_3$  forms two strong methanol–methanol H bonds (paper I) and a strengthened  $\pi$  H bond, thereby producing a greater total binding energy for this structure in the presence of benzene. The  $BM_3$  cluster thus is a particularly clear case in which the presence of the benzene solute changes the lowest-energy H-bonding configuration of its surrounding solvent (methanol trimer).

#### D. $C_6H_6-(CH_3OH)_4$

It is at  $BM_4$  that the dramatic change is seen in both the R2PI and RIDIR spectra, pointing to a significant structural rearrangement. The RIDIR spectrum is dominated by a pair of bands at  $3290$  and  $3321\text{ cm}^{-1}$ , with two barely visible satellite bands at  $3204$  and  $3360\text{ cm}^{-1}$ . Notably absent is any absorption in the  $3500\text{--}3600\text{ cm}^{-1}$  region, which could be



ascribed to a  $\pi$  H-bonded OH stretch transition. The sharp, weak transitions at 3048 and 3101  $cm^{-1}$  are due to the Fermi-resonance split C–H stretch bands of benzene. As in the  $BW_n$  clusters, the C–H stretch bands are unperturbed by the presence of the solvent molecules.

The prediction of the R2PI spectroscopy<sup>14</sup> is that  $BM_4$  binds benzene to a cyclic methanol tetramer. In order to test the RIDIR results against this prediction, the calculated OH stretch infrared frequency shifts and intensities of the methanol tetramer chain 4 [Fig. 7(a)], (3)+1 structure as representative of a branched cycle [Fig. 7(b)], and the tetramer cycle (4) [Fig. 7(c)] are compared with experiment on  $BM_4$ . The qualitative match-up of the experimental spectrum for  $BM_4$  with the calculation for the cyclic  $M_4$  cluster is excellent. Furthermore, recent gas-phase<sup>11</sup> data on  $M_4$  have identified a single OH stretch band at 3290  $cm^{-1}$  (3284  $cm^{-1}$  in a nitrogen matrix<sup>23</sup>) which has been tentatively assigned to the cyclic methanol tetramer. The close correspondence of this transition frequency with the intense pair of bands in  $BM_4$  provides strong evidence for a cyclic  $M_4$  subcluster in  $BM_4$ .

Furthermore, the presence of benzene is expected to distort the OH stretch infrared spectrum from that of cyclic  $M_4$  in precisely the way observed. As discussed in more detail in paper I, the highly symmetric cyclic clusters have OH stretch vibrations which are delocalized around the ring. As is apparent from Fig. 7(c), the infrared spectrum of cyclic  $M_4$  has a degenerate pair of vibrations (with two “nodes” in the phases of the OH oscillators) which carry all the infrared intensity. The OH stretch vibrations above and below this in frequency are forbidden for symmetry reasons, having four and zero nodes, respectively. However, in the presence of benzene, the cyclic structure is distorted away from its high symmetry, thereby partially localizing the OH stretch vibrations. This in turn breaks the degeneracy of the donor OH stretch vibrations and induces intensity in the otherwise forbidden bands above and below the main pair of bands.

This symmetry-breaking effect of benzene has been analyzed recently<sup>20</sup> in some detail in accounting for the RIDIR spectrum of the  $BW_3$  cluster [Fig. 2(B), spectrum (c)]. In that case the benzene– $W_3$  interaction is via a  $\pi$  H bond formed with one of the dangling hydrogens on the cyclic  $W_3$  cluster. The effect on the intensities of the bands is quite dramatic in  $BW_3$ . In contrast, if the methanol tetramer in  $BM_4$  is cyclic, all OH groups in the  $M_4$  subcluster will be involved in H bonding with other methanol molecules. As a result, the interaction of the tetramer cycle with benzene is relegated to benzene–methyl interaction(s) which are weaker than the  $\pi$  H bonds present in  $BW_n$  (or in the chain structures of  $BM_m$  with  $m=1-3$ ). As a result, the symmetry-breaking effect of benzene is lessened. In keeping with this, one observes a 31  $cm^{-1}$  splitting of the degeneracy of the main bands, and only weakly induced intensity in the satellite bands at 3204 and 3360  $cm^{-1}$ . The positions of these weak satellite bands are very near the calculated frequencies for the forbidden bands in  $M_4$  [Fig. 7(c)].

The present data firmly assign the H-bonded architecture in  $BM_4$  as cyclic, just as it is in  $BW_4$ . The *ab initio* results from paper I indicate that the energy difference between cy-

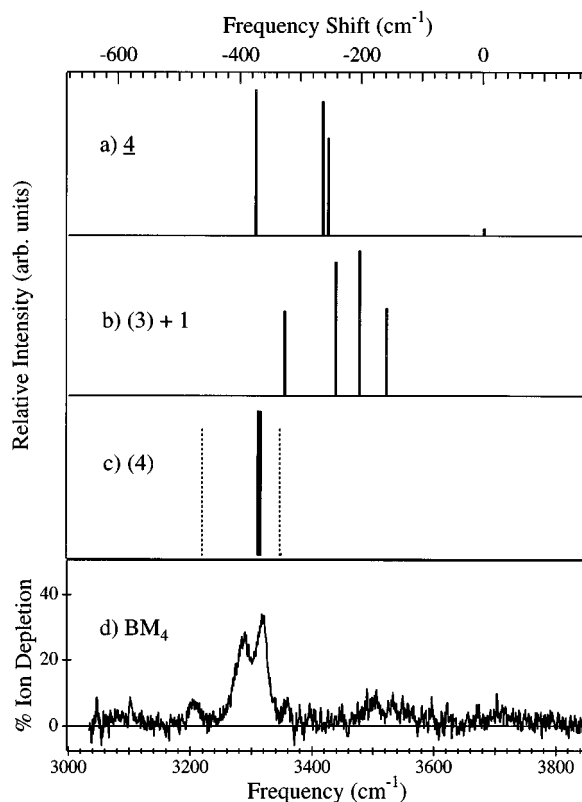


FIG. 7. (a), (b), and (c) *Ab initio* calculated OH stretch harmonic frequency shifts and infrared intensities for the (a) chain, (b) (3)+1 branched-cyclic, and (c) cyclic forms of the free methanol tetramer. In (c), the bold bar indicates the doubly degenerate OH stretch, while the dotted lines locate the positions of the forbidden “satellite” OH stretch fundamentals. (d) RIDIR spectrum of  $BM_4$  for comparison.

clitic and chain structures of  $M_4$  is sizable enough ( $>8$  kcal/mol) that the strong  $\pi$  H bond afforded by the chain structure cannot make up the energy difference. In  $BM_4$ , then, no solvent restructuring occurs as it did in  $BM_3$ .

Although the cyclic structure of  $M_4$  in  $BM_4$  is well-established, what is not well-characterized by the RIDIR spectrum is the orientation or degree of rigidity of the  $M_4$  cycle with respect to the benzene ring. In  $BW_4$ , the  $\pi$  H-bonded OH stretch is clearly observed in the spectrum, ensuring that the cyclic water tetramer interacts with benzene primarily via an out-of-plane interaction. However, in  $BM_4$ , where no dangling OH groups are available for  $\pi$  H bonding, the orientation is less well-defined. Now, armed with the firm structural conclusion for the  $M_4$  subcluster from the RIDIR data, it is worthwhile recalling the R2PI data<sup>14</sup> on  $BM_4$  which more directly probes the interaction of benzene with the  $M_4$  cycle. The electronic frequency shift of the vibronic transitions of the cluster relative to free benzene probes the type of interaction which dominates. A blueshift is consistently associated with a  $\pi$  H-bonding interaction with benzene, while a redshift is found when purely dispersive interactions dominate.<sup>28</sup> Consistent with this, the vibronic transitions of the  $BM_m$  clusters with  $m=1-3$  are 44, 80, and 147 blueshifted from the corresponding transitions in free benzene, respectively. This reflects the increased strength of

the  $\pi$  H bond in these clusters. In  $BM_4$ , the vibronic transitions [Fig. 1(c)] shift dramatically back toward the red to a value only  $19\text{ cm}^{-1}$  above that of free benzene. This is consistent with the loss of  $\pi$  H-bonding interaction in forming cyclic  $M_4$  in  $BM_4$ .

The R2PI spectrum of  $BM_4$  is also notable for its closely spaced, intense set of intermolecular transitions which each vibronic transition of benzene supports. In Fig. 1(c), the entire clump of transitions subtended by the bracket is due to  $BM_4$ , as has been confirmed by IR–UV hole-burning.<sup>24</sup> The presence of many low-frequency intermolecular bands suggests that the  $M_4$  subcluster can librate against benzene with little cost in energy. In a previous paper<sup>14</sup> on the R2PI spectroscopy of  $BM_m$ , OPLS calculations<sup>29</sup> were used to optimize structures for the  $BM_m$  clusters. These predicted that the  $M_4$  subunit interacts with benzene primarily via one methyl group on a single side of benzene, but with  $M_4$  beginning to wrap around the side of benzene. In Fig. 8(a) an alternate structure is shown in which the *ab initio* calculated structure for  $M_4$  acts as a cavity which accepts benzene in an edge-on approach. An interesting feature of this suggested structure is that two of the methyl groups on  $M_4$  interact with opposite sides of the benzene ring, albeit rather weakly due to the small size of the tetramer cavity. Future experiments will need to be designed to test whether this pleasing picture is in fact that taken on by the  $BM_4$  cluster.

### E. $C_6H_6-(CH_3OH)_5$

The RIDIR spectrum of  $BM_5$  reproduced in Fig. 9(b) provides the first look at the OH stretch region of the methanol pentamer, here perturbed by the presence of benzene. No data on the OH spectrum of the gas-phase methanol pentamer is available for comparison; however, Coussan *et al.*<sup>23</sup> attribute the features at  $3260$ ,  $3242$ , and  $3220\text{ cm}^{-1}$  in a nitrogen matrix to  $M_m$  polymers with  $m > 4$ .

As with  $BM_4$ , the spectrum of  $BM_5$  is dominated by broadened band(s) shifted well to the red of the free OH region. The main band is centered at  $3243\text{ cm}^{-1}$ , roughly  $60\text{ cm}^{-1}$  further shifted than the intense transitions in  $BM_4$ , and precisely in the same range as the  $M_m$  polymers observed by Coussan *et al.*<sup>23</sup> ( $3220$ – $3260\text{ cm}^{-1}$ ). A shoulder at  $3286\text{ cm}^{-1}$  is clearly evident in the spectrum of  $BM_5$ , while hints of a further substructure can be seen at  $3171$  and  $3314\text{ cm}^{-1}$ . No  $\pi$  H-bonded OH transition is observed, though a weak, broad feature does appear near  $3500\text{ cm}^{-1}$ , which we attribute to a combination band built on the  $3243\text{ cm}^{-1}$  fundamental. As before, the narrow features at  $3048$  and  $3108\text{ cm}^{-1}$  result from the CH stretch transitions of benzene in the  $BM_5$  cluster.

Figure 9 compares the experimental OH stretch frequencies to those calculated for the cyclic methanol pentamer (5) and the (4)+1 branched cycle from paper I. The other pentamer structures from paper I bear little resemblance to the experimental spectrum and thus have not been included here. Of the calculated spectra, the cyclic pentamer is the best match with experiment; however, the (4)+1 branched cycle also shows some correspondence with experiment. Arguing

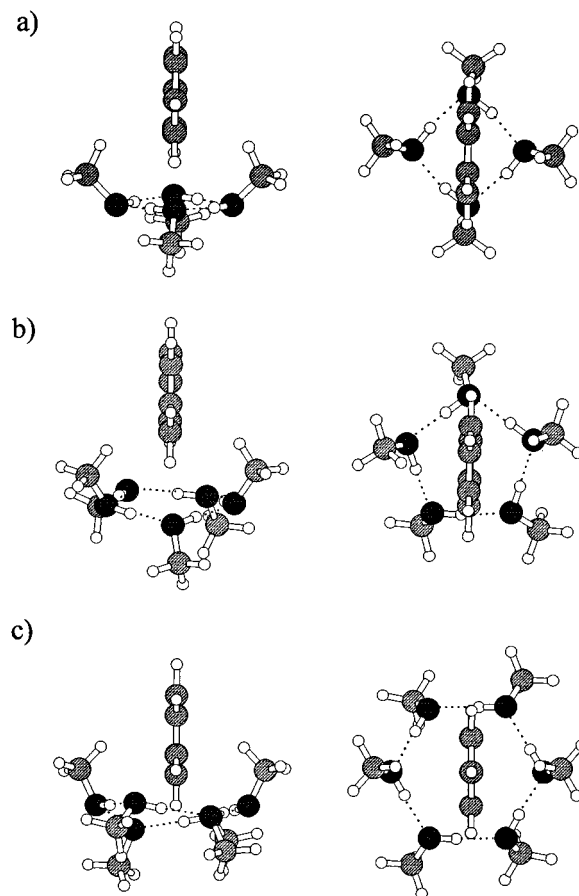


FIG. 8. Schematic pictures of the cyclic “hydrogen-bonding” architectures of (a)  $BM_4$ , (b)  $BM_5$ , and (c)  $BM_6$ . In no case is the orientation of the  $M_m$  cycle with respect to benzene known from experiment. The proposed structure for  $BM_6$  incorporates a boat-shaped  $M_6$  cycle whose nonplanarity induces intensity in otherwise forbidden transitions, qualitatively in keeping with experiment. This boat structure has a cavity which accepts benzene “edge-on” in such a way that the “bow” and “stern” methyl groups interact with opposite sides of the  $\pi$  cloud of benzene.

against this latter structure is the considerably more intense sidebands predicted for (4)+1 than observed experimentally. Given the closer match with (5) and the significantly stronger binding energy calculated for (5) than for (4)+1 (paper I), we tentatively assign the H-bonded architecture of the  $M_5$  cluster in  $BM_5$  as cyclic.

In making this assignment, we correlate the main band at  $3243\text{ cm}^{-1}$  with the near-degenerate pair of transitions in cyclic  $M_5$  which carry the majority of the OH stretch intensity. The shoulder at  $3284\text{ cm}^{-1}$  and (possibly) at  $3314\text{ cm}^{-1}$  match well with the calculated peaks at  $3311$  and  $3324\text{ cm}^{-1}$ , respectively. In cyclic  $M_5$ , these bands gain some intensity both from the asymmetry associated with the odd number of methyl groups in the pentamer ring and from the slight puckering of the ring. Finally, the shoulder at  $3171\text{ cm}^{-1}$  is tentatively assigned to the calculated peak at  $3178\text{ cm}^{-1}$ . In  $BM_5$ , this transition and the shoulders on the blue edge of the main band may gain additional intensity over that predicted in Fig. 9(a) due to the asymmetry provided by complexation to benzene. Such asymmetry causes partial local-

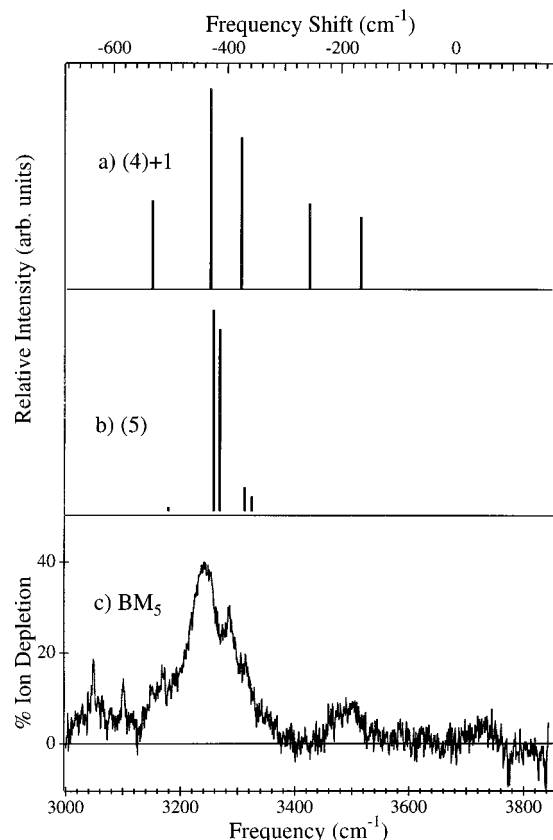


FIG. 9. *Ab initio* OH stretch harmonic frequency shifts and infrared intensities for the (a) (4)+1 branched cyclic and (b) cyclic methanol pentamer. (c) RIDIR spectrum of BM<sub>5</sub> for comparison.

ization in the OH stretch vibrations, thereby altering the intensities of the transitions.

Once again, the orientation of the cyclic M<sub>5</sub> subcluster relative to benzene is not well-established. The R2PI spectrum<sup>14</sup> of BM<sub>5</sub>, which one expects to be sensitive to the orientation of benzene in the cluster, shows an  $S_1 \leftarrow S_0$  frequency shift of  $-19 \text{ cm}^{-1}$  relative to free benzene. This is an additional redshift of  $33 \text{ cm}^{-1}$  relative to that in BM<sub>4</sub>. In our earlier work, OPLS calculations<sup>14</sup> predicted that the M<sub>5</sub> cycle would be positioned on the side of the benzene ring. Figure 8(c) presents a slightly modified version of this structure in which the *ab initio* structure from paper I is used for the cyclic M<sub>5</sub> subcluster rather than the OPLS structure. Note that the expanded size of the pocket in M<sub>5</sub> relative to M<sub>4</sub> may allow stronger methyl- $\pi$  interactions which could shift the electronic transition frequency to the red from that in BM<sub>4</sub>, as observed.

## F. $C_6H_6-(CH_3OH)_6$

The RIDIR spectrum of BM<sub>6</sub> is shown in close-up form in Fig. 10(c). The spectrum provides a first look at the OH stretch region of the methanol hexamer (here perturbed by benzene), since no experimental data on these vibrations of M<sub>6</sub> are available. As with BM<sub>4</sub> and BM<sub>5</sub>, the lack of a  $\pi$  H-bonded peak is strong evidence against a chain or branched-chain structure (paper I). Furthermore, a branched

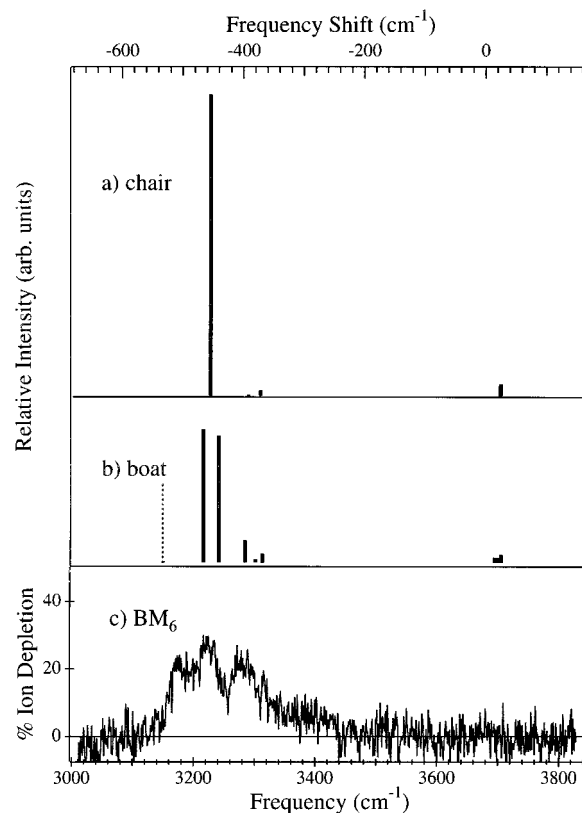


FIG. 10. *Ab initio* OH stretch harmonic frequency shifts and infrared intensities for the (a) chair cyclic, and (b) boat cyclic forms of the free water pentamer. The calculated frequencies have been shifted by  $-81 \text{ cm}^{-1}$  to bring the calculated frequency for the methanol monomer OH stretch into agreement with the experimental (anharmonic) fundamental frequency. (c) RIDIR spectrum of BM<sub>6</sub>. In making the comparison with the W<sub>6</sub> structures, attention is focused on the H-bonded OH stretches of W<sub>6</sub>, since these have a direct analog in the OH stretch modes of M<sub>6</sub>.

cycle would of necessity be a smaller cycle and/or contain a small branch which would have its OH stretch transitions at significantly higher frequencies than those observed ( $\sim 3500 \text{ cm}^{-1}$ ). The remaining structural type is that expected to be most strongly bound; namely, the cyclic methanol hexamer. Once again we make a tentative assignment of BM<sub>6</sub> as containing a cyclic methanol hexamer.

If this assignment is correct, it must also be capable of explaining the substructure present in the RIDIR spectrum, which consists of at least three, and possibly four overlapping bands at 3177, 3224, 3280, and (possibly) 3315  $\text{cm}^{-1}$ . The overall band center in BM<sub>6</sub> is hardly shifted from that in BM<sub>5</sub>, suggesting a saturation in the strength of the H bonds with increasing ring size. This is what is predicted by the OPLS calculations of M<sub>6</sub> by Buck *et al.*,<sup>30</sup> where the average H-bond energy in the cyclic pentamer and hexamer are  $-7.95$  and  $-8.12 \text{ kcal/mol}$ , respectively.

As in the  $m=5$  case, no size-specific experimental data in the OH spectral region of the methanol hexamer exist for comparison to BM<sub>6</sub>. Buck *et al.*<sup>10</sup> have observed two absorptions for M<sub>6</sub> in the CO stretch region at 1041.2 and 1052.5  $\text{cm}^{-1}$ . This is a break in the trend set by the cyclic methanol trimer, tetramer, and pentamer in which only one absorption

TABLE II. Calculated harmonic frequencies<sup>a</sup> and intensities for the chair and distorted boat structures of the water hexamer.

Mode No.	Frequency	Intensity	Symmetry
Chair			
37	3245.6	0.0	A
38	3328.4	2965.8	E
39	3328.4	2965.8	E
40	3391.2	0.5	E
41	3391.2	0.5	E
42	3410.9	91.4	A
43	3806.9	172.4	A
44	3807.0	12.3	E
45	3807.0	12.3	E
46	3807.9	108.5	E
47	3807.9	108.5	E
48	3808.5	4.5	A
Boat			
37	3256.4	4.6	A
38	3322.3	2617.8	B
39	3347.6	2499.6	B
40	3390.8	425.0	A
41	3408.2	51.5	A
42	3419.4	157.3	B
43	3803.7	88.7	B
44	3803.8	63.2	A
45	3808.1	26.4	B
46	3808.5	87.7	A
47	3813.8	147.4	B
48	3813.9	0.6	A

<sup>a</sup>These frequencies have not been shifted relative to the free methanol monomer.

was observed. Monte Carlo and molecular dynamics calculations performed by Buck *et al.*<sup>30</sup> find two nearly degenerate isomers, one with  $S_6$  (chair) and the other with  $C_2$  (boat) symmetry, having binding energies of  $-48.75$  and  $-48.6$  kcal/mol, respectively. The two absorptions in the CO stretch region have been ascribed to nonequivalent methanol environments in a single distorted cyclic  $M_6$  structure.

Due to the size of the  $M_6$  cluster, Becke3LYP/6-31+G\* level calculations were not performed on  $M_6$ . However, calculations of the infrared frequencies and intensities of the chair and boat conformers of the water hexamer (with six less heavy atoms than  $M_6$ ) have been carried out at the same level of theory in the expectation that the H-bonded OH transitions in  $W_6$  will faithfully mimic the qualitative trends in the OH stretch modes of the corresponding conformers of  $M_6$ . Table II summarizes the vibrational data on the chair and boat forms of  $W_6$ . As expected based on the results on the smaller cyclic clusters, essentially all the intensity in the H-bonded OH stretch modes of the chair form is carried by a degenerate pair of transitions at  $3328.4\text{ cm}^{-1}$ . Figure 10(a) shows the calculated spectrum of the  $W_6$  chair when plotted versus frequency shift from the water monomer free OH.<sup>19</sup> By comparison, the experimental spectrum has no single transition dominating the spectrum, but three or four bands which have comparable intensities.

The match-up with the boat form [Fig. 10(b)] is more encouraging. In forming the boat structure [Fig. 8(c)], the planarity of the  $OH\cdots O$  ring is substantially broken. As a

result, even in the absence of benzene, the degeneracy of the central pair is broken, and the forbidden nature of the sidebands is removed. Nevertheless, while the positions of the bands are qualitatively in keeping with the experimental spectrum of  $BM_6$ , the intensities of the sidebands are still too weak. It is reasonable to assume that the sidebands could gain further intensity from the added symmetry-breaking induced by benzene.

Note that the calculated boat conformation is not the lowest-energy boat structure,<sup>30</sup> but one which has the free hydrogens on both "bow and stern" molecules in axial positions. This conformation corresponds with our intuition as to the best binding arrangement of a cyclic  $M_6$  cluster to benzene, as shown in Fig. 8(c). In this conformation of  $M_6$ , the two axial hydrogens of  $W_6$  are replaced by methyl groups which can interact with opposite sides of the benzene ring. The cavity so formed nicely accepts the benzene molecule edge-on, and in fact was the initial basis for thinking that similar conformations could play a role in the  $BM_4$  and  $BM_5$  clusters as well [Figs. 8(a) and 8(b)]. The total binding energy of the  $W_6$  chair and this conformation of the  $W_6$  boat are calculated to be  $-55.66$  and  $-54.16$  kcal/mol, respectively.

The suggestion put forward here is thus that, in the co-expansion of benzene and methanol, the lowest energy  $BM_6$  structure contains a cyclic  $M_6$  subcluster which is distorted into a boat conformation in order to form a better template for maximal interaction with benzene. This distortion maximizes the interaction between benzene and  $M_6$  at the expense of the rearrangement energy from chair to boat conformations of  $M_6$  ( $\sim 1.5$  kcal/mol), much as occurred in favoring chain over cyclic forms of  $M_3$  in  $BM_3$ . In summary, the suggested structure for  $BM_6$  meets an initial test provided by the  $W_6$  calculations, but will require further experimental and theoretical work before a firm assignment is in hand.

Finally, the very different infrared spectra of  $BM_6$  and  $BW_6$  [Figs. 1(A), spectrum (f) and Fig. 1(B), spectrum (f), respectively] and the contrasting structures tentatively assigned to them highlight the unique interactions of water and methanol solvents with benzene. Water hexamer has a number of low energy structures including both cyclic and three-dimensional (3D) cage structures.<sup>20,31</sup> While the cyclic  $W_6$  cluster contains six strong H bonds, the 3D cages form additional H bonds in which some of the water molecules donate both hydrogens to neighboring water molecules. The work of Kim, Jordan, and Zwier<sup>5</sup> compared the structures, binding energies, and OH stretch infrared spectra of the cyclic and two of the lowest energy cagelike  $W_6$  structures with the objective of establishing the water solvent's structure in  $BW_6$ . The comparison clearly established the presence of double-donor water molecules in  $BW_6$ , a result which is consistent only with a 3D cage structure for  $W_6$  in  $BW_6$ . The experimental spectrum best matches the theoretical spectrum of a cage structure containing two double-donating and four single-donating water molecules. Saykally and co-workers<sup>6</sup> have recently made the first experimental detection of precisely this form of  $W_6$  in the far infrared. One can surmise on this basis that benzene does not seem to greatly effect the

structure of  $W_6$ , largely because dangling hydrogens on the 3D cage are still available for  $\pi$  H bonding with benzene.

In the methanol hexamer, the single OH group on each methanol removes the possibility of double donation and produces an energy cost for forming chain or branched-chain structures which have dangling hydrogens available for  $\pi$  H bonding to benzene. The result is a significant energetic preference for cyclic or branched cyclic structures in the larger  $M_m$  clusters, as demonstrated by the calculations on methanol trimer, tetramer, and pentamer in paper I. Thus, in the cyclic methanol hexamer, there is little inducement to break the cycle in complexing with benzene. Yet, the significant flexibility of these larger cyclic clusters can allow distortions which maximize the dispersive interactions with benzene at little cost in H-bonding energy in the  $M_6$  cluster.

Thus, in  $BW_6$ , a stiff  $W_6$  3D cage attaches to benzene via a  $\pi$  H bond involving one of the dangling hydrogens in the structure. This  $\pi$  H bond effectively holds the compact  $W_6$  structure on one face of the benzene ring. In  $BM_6$ , the flexible  $M_6$  cycle interacts weakly with benzene, but can nevertheless deform to accommodate a best interaction with benzene with little cost in energy. We propose a deformation in which the  $M_6$  cycle wraps around the side of the benzene ring [Fig. 8(c)] and interacts with similar strength with both sides of benzene, not unlike the beginnings of a first solvent shell.

### G. The breadths of the OH stretch transitions

The OH stretch transitions in Fig. 2 are those of a single configuration of a finite-sized H-bonded cluster at a few degrees kelvin. The observed breadths serve as a limiting case for comparison with the breadths of the OH stretch spectra in H-bonded liquids and solids.<sup>1,2,7,8</sup>

In the cold, gas-phase  $BW_n$  and  $BM_m$  clusters, the breadths of the transitions show significant dependence on cluster size and type of OH stretch mode. The OH stretch transitions are instrumentally broad in the H-bonded chain structures of  $BM_1$ – $BM_3$ . However, the rearrangement of the  $M_4$  substructure in  $BM_4$  to a cyclic structure is accompanied by an increase in the breadths of the transitions to about 30  $cm^{-1}$  FWHM. Even greater widths are apparent in  $BM_5$  and  $BM_6$ . The *ab initio* calculations of paper I<sup>21</sup> highlight the cooperative strengthening of the H bonds in cyclic  $M_m$  clusters and the delocalization of the OH stretch modes over the OH bonds in the cycle. Both these features would suggest strong coupling of the OH stretch modes to the intermolecular modes associated with the H bonds. Yet, such coupling does not typically produce combination bands in the spectrum, but rather broadens the individual transitions, indicating coupling to a high density of background states. One suspects that the primary coupling of the OH stretch modes may be to the bath of states associated with ring-opened structures involving the breaking of a hydrogen bond (as in a DF trimer<sup>32</sup>) or to dissociative states involving breakup of the cluster (as in a HF trimer<sup>33</sup>). However, a detailed understanding of the magnitudes and sources of the broadening in these clusters is still needed. Nevertheless, the results on

$BW_n$  and  $BM_m$  clusters set a quantitative standard against which dynamical models of mode–mode coupling in H-bonded networks can be tested.

### V. CONCLUSION

The OH stretch vibrations of size-specific benzene–(methanol)<sub>m</sub> ( $m=1$ –6) clusters has been investigated by means of resonant ion-dip infrared spectroscopy. The frequencies and band widths of the observed OH stretch fundamentals are strongly dependent on the structure of the cluster. By comparing the experimental frequencies to both experimental and calculated frequencies of the free methanol clusters, the H-bonding structure in the  $M_m$  subcluster can be firmly assigned.

In  $BM_1$ – $BM_3$ , the structures probed by the present study incorporate one, two, and three methanol molecules in a H-bonded chain whose terminal methanol is  $\pi$  H bonded to benzene. The cooperative strengthening of the  $\pi$  H bond with increasing chain length is evident in the increasing redshift of the  $\pi$  H-bonded OH stretch frequency. By  $BM_3$ , the redshift ( $-92\text{ cm}^{-1}$ ) is nearly as large as the frequency shift of the donor methanol in the free methanol dimer ( $-108\text{ cm}^{-1}$ ).<sup>11</sup> Since the lowest-energy structure for the free methanol trimer is cyclic, the apparent dominance of the chain structure in  $BM_3$  is evidence of a significant structural rearrangement induced by the presence of benzene. In the language of bulk solution, one could say that the benzene molecule has changed the lowest-energy structure taken on by its surrounding solvent.

In  $BM_4$ , the  $M_4$  subcluster is cyclic, the same structure calculated to be lowest in energy in the absence of benzene. In this case, the effect of benzene is much more subtle because the interaction with benzene with a cyclic  $M_m$  cluster is quite weak. The OH stretch spectroscopy reflects the perturbations imposed by benzene in a splitting of the degenerate vibrations which carry all the intensity in  $M_4$ , and a weak inducement of intensity in two otherwise IR-forbidden transitions.

Finally, in  $BM_5$  and  $BM_6$ , the RIDIR spectra show only broadened features centered around  $3200$ – $3250\text{ cm}^{-1}$ , corresponding to frequency shifts of  $450$ – $500\text{ cm}^{-1}$  from the OH stretch fundamental in methanol monomer. The lack of transitions to the blue and the general correspondence with the *ab initio* calculated frequencies of cyclic  $M_5$  and  $W_6$  suggest cyclic  $M_m$  structures for both  $BM_5$  and  $BM_6$ . In  $BM_6$ , the intensity spread and substructure of the OH stretch absorptions are consistent with a distortion of the cyclic  $M_6$  subcluster which breaks degeneracies and turns on transitions which are forbidden in the lowest-energy  $S_6$  symmetry chair structure. We propose the distortion to form a boat structure somewhat analogous to the higher-temperature  $C_2$  structure put forward for  $M_6$  by Buck *et al.*<sup>10,30</sup> in the pure  $M_6$  clusters. In  $BM_6$ , however, we raise the possibility that the “bow and stern” methyl groups are in axial positions. When one brings the benzene molecule up to this structure, the boat forms a cavity for edge-on approach of benzene which can accommodate interactions between the axial methyl groups

and the  $\pi$  cloud on either side of the benzene ring.

The one-for-one comparison of the results on  $BM_m$  with the previous RIDIR spectra<sup>3-5,19</sup> on  $BW_m$  present a series of interesting contrasts all of which arise from the presence of two H-bonding OH groups in water and one in methanol. The spectrum of  $BM_1$  is a single OH stretch transition, while  $BW_1$  has an exceedingly complex set of seven or eight transitions<sup>19</sup> reflecting the large-amplitude torsion and internal rotation of the water molecule in the complex. These motions of  $H_2O$  swap the OH groups involved in the  $\pi$  H bond, and are thus quenched or reduced in  $BM_1$ .  $BW_2$  and  $BM_2$  have similar structures, but in  $BW_3$ , the water trimer is cyclic while the methanol trimer in  $BM_3$  has a chain  $M_3$  structure. Again, the presence of dangling hydrogens in the  $W_3$  cycle enables  $BW_3$  to retain the three highly nonlinear H bonds in  $W_3$  without sacrificing a favorable  $\pi$  H bond with benzene. In contrast, cyclic  $M_3$  ties up all its OH groups in H bonding between methanol molecules, significantly weakening the interaction with benzene's  $\pi$  cloud and favoring formation of the chain structure which retains a cooperatively strengthened  $\pi$  H bond to benzene.

The  $m=4$  and 5 structures of both  $BW_m$  and  $BM_m$  are cyclic, but the spectra of the  $BM_m$  are only slightly perturbed from their  $M_m$  counterparts due to the weak interactions with benzene when all OH groups are tied up in methanol-methanol H bonds.

Finally, the structure of the water hexamer in  $BW_6$  is a three-dimensional cage structure while the methanol hexamer in  $BM_6$  is tentatively assigned as cyclic. The 3D cage is only possible by employing both OH groups in some of the water molecules in H bonds; furthermore, another of the dangling OH groups is involved in  $\pi$  H bonding with benzene. The cyclic  $M_6$  structure uses all OH groups in the cycle. At the same time, the size of the hexamer cycle is sufficient to allow significant conformational flexibility in the cycle with little cost in energy. The tentatively proposed structure for  $BM_6$ , which incorporates a boat-shaped cycle to which benzene binds "edge-on," is reminiscent of the beginnings of a first solvent shell around the benzene solute. In summary, in these small gas-phase benzene/solvent clusters, the tendency of water to self-associate with little deference for benzene and of methanol to rearrange or distort in order to accommodate an increased interaction with benzene at least hints at the molecular-level basis for benzene's immiscibility in water and infinite solubility in methanol.

## ACKNOWLEDGMENT

The authors gratefully acknowledge support for this research from the National Science Foundation (NSF CHE9404716).

- <sup>1</sup>For a recent account, see A. K. Soper and M. G. Phillips, *Chem. Phys.* **107**, 47 (1986), and references therein.
- <sup>2</sup>J. P. Devlin, *Int. Rev. Phys. Chem.* **9**, 29 (1990).
- <sup>3</sup>R. N. Pribble and T. S. Zwier, *Science* **265**, 75 (1994).
- <sup>4</sup>R. N. Pribble and T. S. Zwier, *Faraday Discuss.* **97**, 229 (1994).
- <sup>5</sup>K. Kim, K. D. Jordan, and T. S. Zwier, *J. Am. Chem. Soc.* **116**, 11568 (1994).
- <sup>6</sup>R. J. Saykally (private communication).
- <sup>7</sup>See Refs. 1-8 of paper I.
- <sup>8</sup>See Refs. 9-14 of paper I.
- <sup>9</sup>F. Huisken and M. Stemmler, *Chem. Phys. Lett.* **144**, 391 (1988).
- <sup>10</sup>(a) U. Buck, X. Gu, C. Lauenstein, and A. Rudolph, *J. Phys. Chem.* **92**, 5561 (1988); (b) U. Buck and I. Ettischer, *J. Chem. Phys.* **100**, 6974 (1994).
- <sup>11</sup>F. Huisken, A. Kulcke, C. Laush, and J. M. Lisy, *J. Chem. Phys.* **95**, 3924 (1991).
- <sup>12</sup>B. D. Kay and A. W. Castleman, Jr., *J. Phys. Chem.* **89**, 4867 (1985).
- <sup>13</sup>(a) A. J. Gotch, A. W. Garrett, D. L. Severance, and T. S. Zwier, *Chem. Phys. Lett.* **178**, 121 (1991); (b) A. J. Gotch and T. S. Zwier, *J. Chem. Phys.* **96**, 3388 (1992); (c) A. W. Garrett and T. S. Zwier, *ibid.* **96**, 3402 (1992).
- <sup>14</sup>(a) A. W. Garrett, D. L. Severance, and T. S. Zwier, *J. Chem. Phys.* **96**, 7245 (1992); (b) A. W. Garrett and T. S. Zwier, *ibid.* **92**, 7259 (1992).
- <sup>15</sup>J. Wana, J. A. Menapace, and E. R. Bernstein, *J. Chem. Phys.* **85**, 1795 (1986).
- <sup>16</sup>G. C. Pimentel and A. L. McClellan, *The Hydrogen Bond* (Freeman, San Francisco, 1960).
- <sup>17</sup>*Hydrogen-Bonded Liquids*, edited by J. C. Pore and J. Texeira (Kluwer, Dordrecht, 1991).
- <sup>18</sup>R. J. Jakobsen, J. W. Brasch, and Y. Mikawa, *J. Mol. Struct.* **1**, 309 (1967).
- <sup>19</sup>(a) R. N. Pribble, A. W. Garrett, K. Haber, and T. S. Zwier, *J. Chem. Phys.* **103**, 531 (1995); (b) S. Y. Fredericks, K. D. Jordan, and T. S. Zwier, *J. Phys. Chem.* **100**, 7810 (1996).
- <sup>20</sup>R. H. Page, Y. R. Shen, and Y. T. Lee, *J. Chem. Phys.* **88**, 4621 (1988).
- <sup>21</sup>F. Hagemester and T. S. Zwier (unpublished).
- <sup>22</sup>W. Scherzer, H. L. Selzle, and E. W. Schlag, *Chem. Phys. Lett.* **195**, 11 (1992); W. Scherzer, O. Kratzschmar, H. Selzle, and E. W. Schlag, *Z. Naturforsch.* **47a**, 1248 (1992).
- <sup>23</sup>S. Coussan, N. Bakkas, A. Loutellier, J. P. Perchard, and S. Racine, *Chem. Phys. Lett.* **217**, 123 (1994).
- <sup>24</sup>R. N. Pribble and T. S. Zwier (unpublished results).
- <sup>25</sup>H.-D. Barth and B. Brutschy, *Z. Phys. Chem.* (in press).
- <sup>26</sup>L. Schriver, A. Burneau, and J. P. Perchard, *J. Chem. Phys.* **77**, 4926 (1982).
- <sup>27</sup>O. Schrems, *J. Mol. Struct.* **141**, 451 (1986).
- <sup>28</sup>A. W. Garrett and T. S. Zwier, in *Advances in Multiphoton Processes and Spectroscopy*, edited by S. H. Lin, A. A. Villaeys, and Y. Fujimara (World Scientific, Singapore, 1994), Vol. 8, Part 2, pp. 129-188.
- <sup>29</sup>OPLS potentials have optimized parameters for liquid simulations, and are semiempirical electrostatic potentials. See (a) W. L. Jorgenson, *J. Am. Chem. Soc.* **103**, 341 (1981); (b) *J. Phys. Chem.* **90**, 1276 (1986).
- <sup>30</sup>(a) U. Buck, B. Schmidt, and J. G. Siebers, *J. Chem. Phys.* **99**, 9428 (1993); (b) U. Buck and B. Schmidt, *ibid.* **98**, 9410 (1993).
- <sup>31</sup>C. J. Tsai and K. D. Jordan, *Chem. Phys. Lett.* **213**, 181 (1993).
- <sup>32</sup>D. J. Nesbitt, in *Reactions in Clusters and Condensed Phases*, edited by J. Jortner (Kluwer, Netherlands, 1994), p. 137.
- <sup>33</sup>D. W. Michael and J. M. Lisy, *J. Chem. Phys.* **85**, 2528 (1986).